

UC Santa Barbara

UC Santa Barbara Previously Published Works

Title

Tree mortality predicted from drought-induced vascular damage

Permalink

<https://escholarship.org/uc/item/55b5v4q8>

Journal

Nature Geoscience, 8(5)

ISSN

1752-0894

Authors

Anderegg, WRL
Flint, A
Huang, CY
et al.

Publication Date

2015-05-30

DOI

10.1038/ngeo2400

Peer reviewed

Tree mortality predicted from drought-induced vascular damage

William R. L. Anderegg^{1*}, Alan Flint², Cho-ying Huang³, Lorraine Flint², Joseph A. Berry⁴, Frank W. Davis⁵, John S. Sperry⁶ and Christopher B. Field⁴

The projected responses of forest ecosystems to warming and drying associated with twenty-first-century climate change vary widely from resiliency to widespread tree mortality^{1–3}. Current vegetation models lack the ability to account for mortality of overstorey trees during extreme drought owing to uncertainties in mechanisms and thresholds causing mortality^{4,5}. Here we assess the causes of tree mortality, using field measurements of branch hydraulic conductivity during ongoing mortality in *Populus tremuloides* in the southwestern United States and a detailed plant hydraulics model. We identify a lethal plant water stress threshold that corresponds with a loss of vascular transport capacity from air entry into the xylem. We then use this hydraulic-based threshold to simulate forest dieback during historical drought, and compare predictions against three independent mortality data sets. The hydraulic threshold predicted with 75% accuracy regional patterns of tree mortality as found in field plots and mortality maps derived from Landsat imagery. In a high-emissions scenario, climate models project that drought stress will exceed the observed mortality threshold in the southwestern United States by the 2050s. Our approach provides a powerful and tractable way of incorporating tree mortality into vegetation models to resolve uncertainty over the fate of forest ecosystems in a changing climate.

Forests play a central role in global water, energy and biogeochemical cycles and provide substantial ecosystem services to societies around the globe⁶. Yet the fate of forest ecosystems in a changing climate is highly uncertain. Rising atmospheric CO₂ concentrations may benefit trees, particularly through increasing water-use efficiency⁷, but concomitant increases in temperature and drought stress could potentially overwhelm these benefits, leading to widespread forest dieback in many ecosystems globally⁸. Although precipitation projections under climate scenarios are more variable and uncertain, general circulation models project consistent increases in air temperature and thus evaporation over much of the world and resulting decreases in soil moisture in many regions, leading to more intense and frequent droughts⁹. Recent studies have indicated resilience in forest biomes in response to early twenty-first-century droughts through inter-annual modulations in water-use efficiency¹⁰ and long-term increases in forest water-use efficiency⁷. In contrast, severe regional droughts have strongly decreased the carbon sink of key forest ecosystems^{11–13} and widespread, climate-induced tree mortality has been observed around the globe^{8,14}.

The balance of resiliency versus the potential for widespread forest dieback due to climatic extremes hinges in large part on poorly understood demographic processes, which are not well represented in most dynamic global vegetation models (DGVMs). An increase in mortality rate can be as important as a change in productivity for carbon sinks¹⁵. Application of DGVMs to known severe drought stress in controlled rainfall exclusion experiments reveals that they do not accurately capture drought-induced forest dieback⁵. Thus, there is a compelling need for an approach to simulate spatial and temporal patterns of tree mortality and to test model predictions against regional mortality data sets, such as remote-sensing estimates¹⁶. This can then be a foundation for incorporating mortality algorithms into vegetation models that can be trusted for future projections of change, for instance when coupled to global circulation models.

Trees die from drought and temperature stress through complex and poorly understood pathways of interrelated physiological failures that often interact with biotic agents^{4,17}. Hydraulic failure through xylem cavitation has been shown to be a major mortality mechanism across a number of angiosperm species^{18–20}. Using a combination of field physiological measurements, a plant hydraulic model²¹, a hydrologic model²², climate projections and multiple mortality data sets (Supplementary Fig. 1), we tested: does a hydraulic threshold as a function of drought stress emerge across forest sites during ongoing tree mortality; can this mechanistic-based threshold be used to hindcast patterns of mortality with reasonable accuracy compared to multiple mortality data sets; and what do global circulation model projections suggest for future trajectories of this drought stress and exceedance frequency of a mortality threshold? We examined a recent widespread, climate-induced forest die-off of trembling aspen (*Populus tremuloides*; hereafter aspen) in 91,500 Ha in the southwestern United States. As the most widely distributed tree species in North America with major economic and ecological value²³, aspen presents an ideal test case for modelling tree mortality.

We quantified drought stress as climatic water deficit²⁴ (CWD)—the difference between plant water demand, which is determined by atmospheric water demand (here, potential evapotranspiration, PET), and plant water supply, which is determined in part by available soil moisture (here, actual evapotranspiration, AET). Owing to low precipitation and high temperatures, CWD reached peak values around 2000–2003, representing the severe drought that initiated ongoing tree mortality (Fig. 1).

¹Department of Ecology and Evolutionary Biology, Guyot Hall, Princeton University, Princeton, New Jersey 08540, USA. ²United States Geological Survey, Sacramento, California 95819, USA. ³Department of Geography, National Taiwan University, Taipei 10617, Taiwan. ⁴Department of Global Ecology, Carnegie Institution for Science, Stanford, California 94305, USA. ⁵Bren School of Environmental Science and Management, 2400 Bren Hall, University of California, Santa Barbara, California 93106, USA. ⁶Department of Biology, University of Utah, Salt Lake City, Utah 84112, USA.

*e-mail: anderegg@princeton.edu

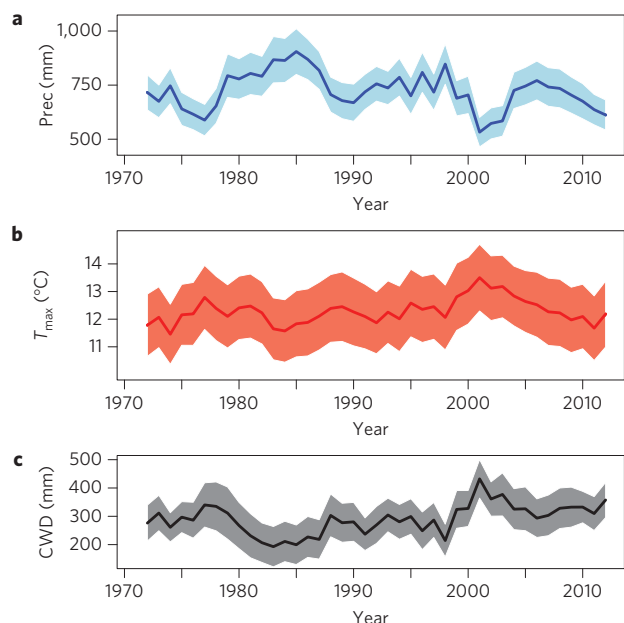


Figure 1 | Hydrologic model simulations. a–c. Three-year running mean (solid line) ± 1 s.d. (shading) of annual precipitation (**a**) and mean maximum daily temperature per month averaged over the year from Parameter-elevation Regressions on Independent Slopes Model (PRISM) 800 m climate data (**b**), and modelled annual CWD from the Basin Characterization Model²² (**c**) across the 87 field aspen stands in the study region in Colorado, USA from 1970–2013.

We used field measurements of plant hydraulic conductance to test for a potential threshold as a function of accumulated CWD from 2000–2013. As native branch hydraulic conductivity has been found to predict aspen stem mortality across years²⁰, providing an indicator of tree hydraulic health, we tested for a threshold in hydraulic conductivity over a large spatial gradient that included both healthy and dying stands. We found a threshold during ongoing mortality where hydraulic conductivity fell rapidly as a function of accumulated CWD (Fig. 2a). The value of modelled CWD where the field-measured hydraulic threshold occurred, which was identified using a standard numerical algorithm to calculate the break-point in a segmented regression²⁵, was similar from branches sampled during multiple years (Fig. 2a). This field-derived hydraulic threshold coincided with a nonlinear increase in regional percentage of aspen mortality as a function of CWD (Fig. 2b, shaded), indicating that this threshold is probably mechanistically linked to mortality.

To determine whether the hydraulic threshold could be explained by the vulnerability of aspen xylem to drought-induced xylem cavitation, we used a detailed plant hydraulic model²¹ that predicts the loss of tree water conducting capacity as a function of soil water availability and xylem vulnerability. The model accurately captured published patterns in whole-tree hydraulic conductance in both healthy and dying stands ($R^2 = 0.91$, $p < 0.001$), as well as the decline and death of ramets (Supplementary Figs 2 and 3). Simulations using modelled monthly soil moisture from 2000–2013 at the field sites where soil characteristics had been measured revealed a strong relationship between CWD and time spent at high percent loss of hydraulic conductivity (Supplementary Fig. 4), indicated previously as a useful mortality predictor variable²⁶. Furthermore, high canopy mortality occurred at a threshold CWD value similar to that observed in branch conductivities (Supplementary Fig. 4). This supports the hypothesis that low tree and branch conductivities seem to initially result from xylem cavitation during drought years, although other factors probably come into play to explain

why these conductances might remain depressed for multiple years post-drought²⁰.

Using the 2010–2011 field-derived hydraulic threshold (CWD: $5,470 \pm 153$ mm (s.e.m.)) for mortality, CWD simulations from the hydrologic model effectively captured both broad spatial patterns (Fig. 3a) and finer topographically driven variation in satellite estimates of severe mortality (Fig. 3b). Total hindcast accuracy (correct classifications of dead and healthy/total points) was 75% (Supplementary Table 1). Tests against two additional mortality data sets—an independent set of 57 field plots and digitized polygons collected by the US Forest Service aerial surveys—yielded similar estimates of model accuracy (Supplementary Tables 2 and 3). CWD predicted spatial patterns of mortality with much higher accuracy than soil moisture or climate variables alone (Supplementary Table 4). Hindcast accuracy was highest on the western side of the forest (Fig. 3a), where the greatest abundance of aspen forest occurs, and less accurate in high elevations and the southeastern corner of the region (Fig. 3a). Sensitivity analysis on varying the lethal CWD levels indicated that the hydraulic-CWD threshold was within 1–3% of the best balance of sensitivity and specificity, and a synthetic performance metric (Supplementary Tables 1–3).

Simulations of CWD from 2007–2100 using the Coupled Model Intercomparison Project—Phase 5 (CMIP5) climate models revealed that CWD is projected to increase for all models except CanESM2 in the lower-concentrations scenario (Representative Concentration Pathway 4.5 (RCP 4.5); Fig. 4 and Supplementary Fig. 8). Four of the six models exceeded the hydraulic threshold identified in Fig. 2a in the second half of the twenty-first century in the lower-concentrations scenario, although model spread was large (Fig. 4). In the higher-concentrations scenario, CWD increases in all models and crosses the hydraulic mortality threshold on average around 2050 (Fig. 4). These projections reveal that the temperature-driven increases in PET are likely to cause increasing drought stress in this region, with large areas of aspen forest frequently exceeding the threshold that triggered mortality by the 2050s.

Our results highlight that hydraulic properties can influence species' distribution boundaries and, as such, may prove valuable in forecasting drought-induced tree mortality. For example, our model captured the high prevalence of aspen mortality on southern and western boundaries of aspen distribution in this region (Fig. 3b) and important topographic patterns of higher mortality on south- and west-facing slopes (Fig. 3a). Although the absolute value of the hydraulic-based threshold could vary geographically, sensitivity analyses of the current model parameterization indicate that the field-measured threshold was robust and near the best-fitting model (Supplementary Tables 1–3).

Empirical relationships between climate variables and tree mortality have been used to illuminate the key sensitivities of forests to different characteristics of drought, such as vapour pressure deficit versus precipitation deficit²⁷. Our analysis moves beyond empirical relationships, however, because we have forged a link between hydroclimatic stress and physiological stress to generate cross-scale (tree-to-region) predictions of widespread tree mortality based on a plant's vulnerability to cavitation and test these predictions against three mortality data sets. Tree hydraulic traits have been associated with degree of mortality in multiple ecosystems, primarily in angiosperms^{13,18}. Carbon metabolism and biotic agent attack (for example, bark beetles) are also probably important in some cases⁴, notably in more isohydric gymnosperms that dominate some boreal and temperate regions, and plant carbon status and vascular health are probably interdependent⁴. Given the ability to model vascular capacities as a function of climate and the dependence of plant health on vascular health^{4,18}, the hydraulic threshold concept may prove generally useful in capturing the vulnerability of angiosperm forests to drought in many ecosystems²⁸.

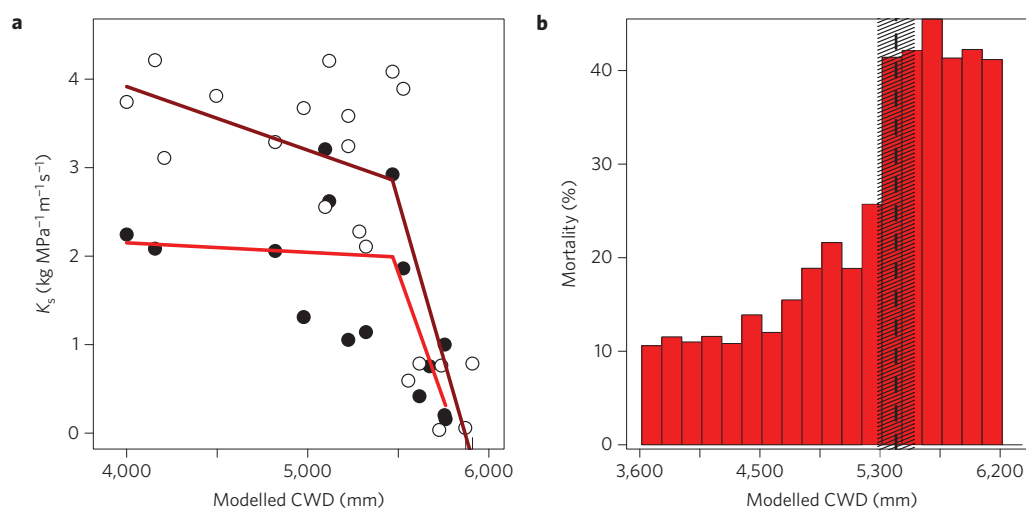


Figure 2 | Plant hydraulic threshold in relation to water deficit. **a**, Combined 2010 and 2011 (filled symbols) and 2013 field measurements (open symbols) of basal area-specific branch hydraulic conductivity for aspen stands as a function of modelled CWD during the drought period. Red lines indicate the break-point regression best fit for 2010–2011 data (red) and 2013 data (dark red). **b**, Percentage of remotely sensed pixels experiencing severe mortality (>50% canopy mortality) as a function of modelled CWD. The dashed line indicates the hydraulic threshold from **a**, with shading for ± 1 standard error in the threshold.

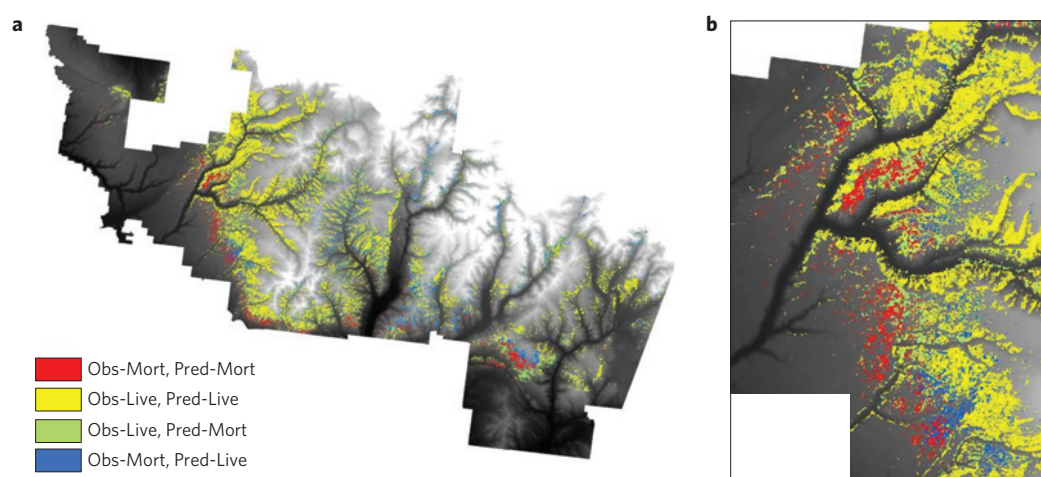


Figure 3 | Hindcast maps of forest mortality. **a, b**, Colours indicate differences between predicted mortality based on the hydraulic threshold and modelled CWD from the hydrologic model and observed severe aspen mortality (>50% canopy mortality) based on Landsat estimates—Observed Mort, Predicted Mort (red); Observed Live, Predicted Live (yellow); Observed Live, Predicted Mort (green); Observed Mort, Predicted Live (blue)—for the whole San Juan National Forest (**a**) and a ~20,000 Ha sub-region of the study area (centre latitude: 37.3° N; longitude: 108.2° W; **b**). Black-white background is a digital elevation model from low (black) to high (white) elevation.

The accumulated deficit between plant water demand and supply provides an attractive link between drought, species physiology and tree mortality. It incorporates both atmospheric water demand and available soil moisture reserves through soil moisture-limited evapotranspiration. Furthermore, both PET and AET are readily calculated within current land-surface models, and thus estimating CWD in these models is straightforward. Differences in drought vulnerability between species or between plant functional types could be incorporated both through modifications of a hydraulic threshold by plant functional traits¹⁸ and through modifications in simulated AET across species and biomes. For example, deep rooting depths in tropical tree species would allow sustained AET during drought, avoiding lethal CWD values until later in drought. Our results provide a foundation for including plant hydraulic conductivity (K_s) and xylem water potential (Ψ_x) in land-surface models where plant hydraulics predict AET and vascular health as a function of climate, soil and key plant traits, such as rooting depth,

vulnerability to cavitation, repair capability and root/leaf ratios. Thus, although the analyses presented here are specific to a single species and region, and a single CWD threshold is unlikely across ecosystems, we find that a great deal can be learnt from modelling tree mortality with simple approaches, which seem promising for incorporating first-order estimates of drought-mediated tree mortality into DGVMs. Aspen exemplifies a fast-growing broad-leaved deciduous temperate plant functional type in these models, and is considered relatively anisohydric in its stomatal control. Our results are most likely applicable to similar species.

Ultimately, a better understanding of the physiology and processes that mediate demographic parameters at large scales is needed to project forest ecosystems' response to climate change. Algorithms based on these processes are most useful if they are computationally tractable enough to be incorporated into land-surface models, theoretically sound, and effectively capture physiological differences across species and plant functional types. The

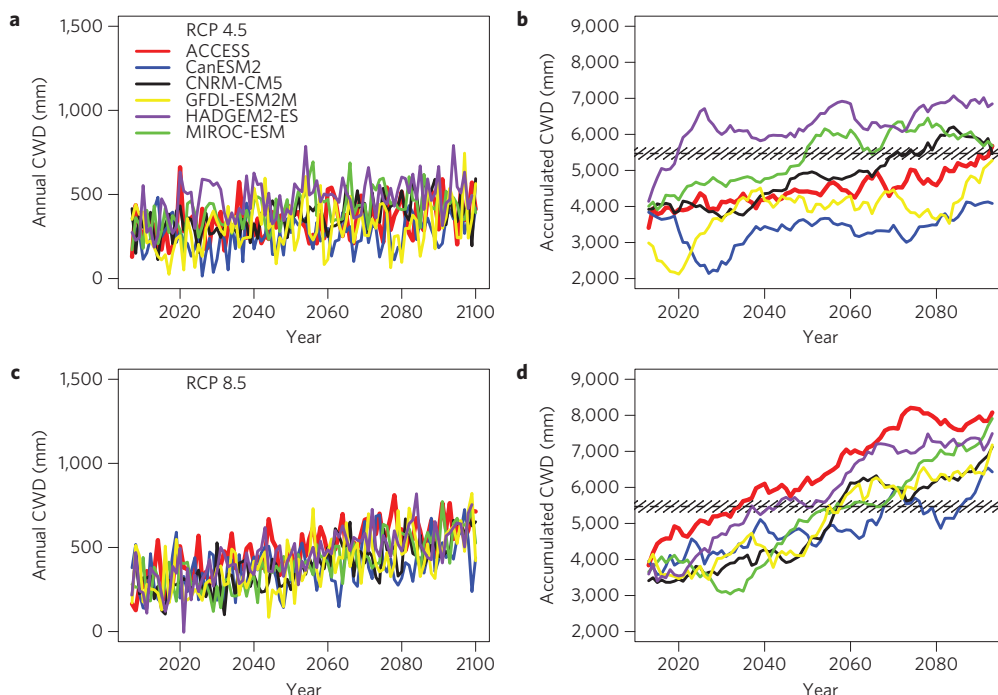


Figure 4 | Future trajectories of drought stress. Hydrologic model simulations of CWD when forced by six general circulation models from the CMIP5 multi-model archive for a lower (RCP 4.5) and higher (RCP 8.5) climate scenario for the 87 aspen field sites. **a**, Simulations of annual CWD for RCP 4.5. **b**, CWD accumulated over 14 years and the dashed line and shading represents the mortality threshold ± 1 standard error from Fig. 2a. **c**, Simulations of annual CWD for RCP 8.5. **d**, CWD accumulated as in **b** for RCP 8.5. The legend in **a** applies to all panels.

difference between plant water demand and supply, and its linkage to hydraulic impairment by xylem cavitation, shows substantial promise for predicting forest mortality with climate change.

Methods

We used simulations of CWD from a high-resolution hydrologic model (the Basin Characterization Model²²) from 1970–2013 to hindcast aspen mortality patterns across 91,500 Ha in southwestern Colorado, USA. Aspen mortality has been documented across the western United States and Canada following a severe drought beginning in 2000 (ref. 23). We used field measurements of branch hydraulic conductivity during ongoing mortality and simulations with a detailed plant hydraulics model to interpret and gain insight into lethal levels in CWD calculated over 2000–2013 during which a pixel of forest was likely to have experienced mortality. Branch segments ($n = 104$) were acquired from 33 aspen stands across a broad array of topography and hydraulic conductivity was measured via a standard protocol²⁹. A detailed plant hydraulics model²¹ was parameterized using published vulnerability-to-cavitation curves and extensive branch and whole-tree hydraulic data from aspen trees of the study region and then evaluated against published estimates of transpiration and whole-tree hydraulic conductance in three aspen stands. This model was then used to examine levels of CWD above which mortality occurred by calculating the time spent at high percent loss of conductivity from cavitation and soil drying, indicated as being a key mortality predictor variable in a previous multi-model comparison study that included this hydraulic model²⁶. Using the field-derived threshold in CWD ($5,470 \pm 153$ mm), we then compared predictions of ‘mortality likely’ areas to three mortality data sets: published high-resolution remotely sensed maps of mortality severity generated using Landsat imagery³⁰; polygons of high mortality determined via aerial surveys; and an independent set of 57 field sites distributed throughout the region. We assessed mortality hindcast performance with total accuracy, sensitivity, specificity, and area under receiver operating curve, and performed extensive sensitivity analyses in the mortality threshold (Supplementary Tables 1–3).

Code availability. The code is not available.

Received 30 December 2014; accepted 27 February 2015;
published online 30 March 2015

References

1. Cox, P. M. *et al.* Amazonian forest dieback under climate-carbon cycle projections for the 21st century. *Theor. Appl. Clim.* **78**, 137–156 (2004).

2. Scholze, M., Knorr, W., Arnell, N. W. & Prentice, I. C. A climate-change risk analysis for world ecosystems. *Proc. Natl Acad. Sci. USA* **103**, 13116–13120 (2006).
3. Huntingford, C. *et al.* Simulated resilience of tropical rainforests to CO₂-induced climate change. *Nature Geosci.* **6**, 268–273 (2013).
4. McDowell, N. G. *et al.* The interdependence of mechanisms underlying climate-driven vegetation mortality. *Trends Ecol. Evol.* **26**, 523–532 (2011).
5. Powell, T. L. *et al.* Confronting model predictions of carbon fluxes with measurements of Amazon forests subjected to experimental drought. *New Phytol.* **200**, 350–365 (2013).
6. Bonan, G. B. Forests and climate change: Forcings, feedbacks, and the climate benefits of forests. *Science* **320**, 1444–1449 (2008).
7. Keenan, T. F. *et al.* Increase in forest water-use efficiency as atmospheric carbon dioxide concentrations rise. *Nature* **499**, 324–327 (2013).
8. Allen, C. D. *et al.* A global overview of drought and heat-induced tree mortality reveals emerging climate change risks for forests. *Forest Ecol. Manage.* **259**, 660–684 (2010).
9. Stocker, T. F. *et al.* (eds) *Climate Change 2013: The Physical Science Basis* (IPCC, Cambridge Univ. Press, 2013).
10. Ponce-Campos, G. E. *et al.* Ecosystem resilience despite large-scale altered hydroclimatic conditions. *Nature* **494**, 349–352 (2013).
11. Zhao, M. & Running, S. W. Drought-induced reduction in global terrestrial net primary production from 2000 through 2009. *Science* **329**, 940–943 (2010).
12. Ma, Z. *et al.* Regional drought-induced reduction in the biomass carbon sink of Canada’s boreal forests. *Proc. Natl Acad. Sci. USA* **109**, 2423–2427 (2012).
13. Phillips, O. L. *et al.* Drought-mortality relationships for tropical forests. *New Phytol.* **187**, 631–646 (2010).
14. van Mantgem, P. J. *et al.* Widespread increase of tree mortality rates in the Western United States. *Science* **323**, 521–524 (2009).
15. Friend, A. D. *et al.* Carbon residence time dominates uncertainty in terrestrial vegetation responses to future climate and atmospheric CO₂. *Proc. Natl Acad. Sci. USA* **111**, 3280–3285 (2014).
16. Anderegg, W. R. L., Berry, J. A. & Field, C. B. Linking definitions, mechanisms, and modeling of drought-induced tree death. *Trends Plant Sci.* **17**, 693–700 (2012).
17. Sala, A., Piper, F. & Hoch, G. Physiological mechanisms of drought-induced tree mortality are far from being resolved. *New Phytol.* **186**, 274–281 (2010).
18. Hoffmann, W. A., Marchin, R. M., Abit, P. & Lau, O. L. Hydraulic failure and tree dieback are associated with high wood density in a temperate forest under extreme drought. *Glob. Change Biol.* **17**, 2731–2742 (2011).

19. Urli, M. *et al.* Xylem embolism threshold for catastrophic hydraulic failure in angiosperm trees. *Tree Phys.* **33**, 672–683 (2013).
20. Anderegg, W. R. L. *et al.* Drought's legacy: multiyear hydraulic deterioration underlies widespread aspen forest die-off and portends increased future risk. *Glob. Change Biol.* **19**, 1188–1196 (2013).
21. Sperry, J. S., Adler, F. R., Campbell, G. S. & Comstock, J. P. Limitation of plant water use by rhizosphere and xylem conductance: Results from a model. *Plant Cell Environ.* **21**, 347–359 (1998).
22. Flint, L. E., Flint, A. L., Thorne, J. H. & Boynton, R. Fine-scale hydrologic modeling for regional landscape applications: The California Basin Characterization Model development and performance. *Ecol. Process.* **2**, 1–21 (2013).
23. Rehfeldt, G. E., Ferguson, D. E. & Crookston, N. L. Aspen, climate, and sudden decline in western USA. *Forest Ecol. Manage.* **258**, 2353–2364 (2009).
24. Stephenson, N. Actual evapotranspiration and deficit: Biologically meaningful correlates of vegetation distribution across spatial scales. *J. Biogeogr.* **25**, 855–870 (1998).
25. Muggeo, V. M. Estimating regression models with unknown break-points. *Stat. Med.* **22**, 3055–3071 (2003).
26. McDowell, N. G. *et al.* Evaluating theories of drought-induced vegetation mortality using a multimodel—experiment framework. *New Phytol.* **200**, 304–321 (2013).
27. Park Williams, A. *et al.* Temperature as a potent driver of regional forest drought stress and tree mortality. *Nature Clim. Change* **3**, 292–297 (2013).
28. Choat, B. *et al.* Global convergence in the vulnerability of forests to drought. *Nature* **491**, 752–755 (2012).
29. Sperry, J. S., Donnelly, J. R. & Tyree, M. T. A method for measuring hydraulic conductivity and embolism in xylem. *Plant Cell Environ.* **11**, 35–40 (1988).
30. Huang, C.-Y. & Anderegg, W. R. L. Large drought-induced aboveground live biomass losses in southern Rocky Mountain aspen forests. *Glob. Change Biol.* **18**, 1016–1027 (2012).

Acknowledgements

W.R.L.A. thanks the NSF DDIG grant for research funding and equipment. W.R.L.A. was supported in part by the NOAA Climate and Global Change Postdoctoral Fellowship program and an award from the Department of Energy (DOE) Office of Science Graduate Fellowship Program (DOE SCGF). C.-y.H. was sponsored by the Ministry of Science and Technology of Taiwan and National Taiwan University. F.W.D. was supported in part by the National Science Foundation Macrosystems Biology Program, NSF no. EF-1065864. J.A.B. and C.B.F. were supported by the Carnegie Institution for Science. We acknowledge the World Climate Research Programme's Working Group on Coupled Modelling, which is responsible for CMIP, and we thank the climate modelling groups (listed in Methods of this paper) for producing and making available their model output. For CMIP the US Department of Energy's Program for Climate Model Diagnosis and Intercomparison provides coordinating support and led development of software infrastructure in partnership with the Global Organization for Earth System Science Portals.

Author contributions

W.R.L.A., J.A.B. and C.B.F. conceived the experiment. W.R.L.A. collected the data and W.R.L.A. and A.F. ran the models. C.-y.H., L.F., F.W.D. and J.S.S. contributed new analytic tools. W.R.L.A. wrote the paper with all authors adding revisions.

Additional information

Supplementary information is available in the [online version of the paper](#). Reprints and permissions information is available online at www.nature.com/reprints. Correspondence and requests for materials should be addressed to W.R.L.A.

Competing financial interests

The authors declare no competing financial interests.